ELSEVIER

Thermochimica Acta 401 (2003) 111–119

thermochimica acta

www.elsevier.com/locate/tca

Micro-thermal analysis of NiTi shape memory alloy thin films

Jianxin Zhang [a], Nicholas W. Botterill [b], Clive J. Roberts [a,*], David M. Grant [b]

[a] *Laboratory of Biophysics and Surface Analysis, School of Pharmaceutical Sciences, University of Nottingham, Nottingham NG7 2RD, UK*
[b] *School of Mechanical, Materials and Manufacturing and Management, University of Nottingham, Nottingham NG7 2RD, UK*

Received 1 July 2002; received in revised form 4 October 2002; accepted 14 October 2002

Abstract

A novel technique of micro-thermal analysis (micro-TA) has been used to investigate martensitic to austenitic transformations of near equi-atomic NiTi shape memory alloy (SMA) thin films deposited on silicon wafer by a plasma assisted sputter deposition technique. The results demonstrate that both power and sensor deflection signal of the technique, equivalent to micro-differential thermal analysis (μDTA) and micro-thermomechanical analysis (μTMA), respectively, have a capability of locally characterising transformation temperatures of the SMA films. The phase transition temperatures can be identified as an abrupt deviation of power and thermal expansion from linearity. The change in probe deflection reveals a sample contraction of 0.44% following the martensite to austenitic transformation. This dimension change is consistent with the difference in the unit cell volumes of the different phases. The individual films investigated here show a spatial variation on the micron-scale in the martensite to austenite transition temperatures as the surface is probed. A possible reason for this may lie in the inhomogeneous distribution of Ti and Ni in the film structure as the transition temperature is very sensitive to composition, showing typically a 100 K temperature change between 50 and 51 at.% Ni in Ti. Conventional bulk DSC experiments were carried out on the same materials and the results were compared with those from the micro-TA.

Keywords: Micro-thermal analysis; Scanning thermal microscopy; Shape memory alloy; Phase transformation

1. Introduction

In recent years, significant progress has been made on the development of scanning thermal microscopy (SThM) to study and image thermal properties of materials at the micro-scale [1–6]. The basic principle of SThM is to replace the conventional tip of atomic force microscopy (AFM) with a thermal sensor. The most common and useful thermal sensor is a sharpened, V-shaped resistive Wollaston wire which was developed by Dinwiddie et al. [4] and subsequently used by, amongst others, Hammiche et al. [5,6]. With the Wollaston-wire probe, not only topographic and thermal images but also localised thermal analysis (LTA) with approximately a micrometer spatial resolution may be recorded. In addition, subsurface information could also be obtained by incorporating a temperature modulation technique developed by Hammiche et al. [6], which is analogous to modulated temperature differential scanning calorimetry (MTDSC) [7]. A commercial version of this probe within a modified AFM was introduced in 1998 by TA Instruments (Micro-Thermal Analyser, μTA™ 2990).

The introduction of micro-thermal analysis (micro-TA) has demonstrated significant opportunities in characterising materials such as polymers, composites, pharmaceuticals and metals. Price and colleagues

* Corresponding author. Fax: +44-01559515110.
E-mail address: clive.roberts@nottingham.ac.uk (C.J. Roberts).

0040-6031/03/$ – see front matter © 2002 Elsevier Science B.V. All rights reserved.
PII: S0040-6031(02)00502-6

have successfully identified components in a multiplayer polymer packaging film [8], phase separation of polymer blends, a melting temperature of the wax layer on a leaf [9], and the active and inert components of pharmaceuticals [10,11]. Similarly, micro-TA was also employed to examine the drug mixture of ibuprofen/HPMC E4M by Royall et al. [12], and distinguish two polymorphs of the drug cimetidine by Sanders et al. [13]. Bond et al. [14] have also compared micro-TA and differential scanning calorimetry (DSC) analysis of pyridoxal hydrochloride, and two commonly used pharmaceutical excipients, Mannitol and Avicel. SThM imaging alone has been used to follow the spinodal decomposition processes of a miscible polymer blend of poly(vinyl methyl ether)/polystyrene [15]. LTA analysis has been used to determine the thickness effect of deposited ultrathin polystyrene films on their glass transition temperatures [16]. LTA can be considered as a quantitative measurement if an appropriate calibration method is utilised, and therefore is more attractive than SThM imaging alone to material scientists. Other applications include characterisation of polymer composite interfaces [17], measurement of localised thermal conductivity of different materials [18]. A recent review in this subject can be found in [19].

Since its discovery in 1962 [20], the shape memory effect in NiTi has prompted a wide range of applications due to its ability to recover from up to 10% strain, with recovery stresses approaching 400 MPa. The memory properties that are of most interest are the ability of the alloy to return to a predetermined shape upon heating, the force that is generated and the mechanical work that can be done by the alloy as it regains its shape; hence the first applications were thermal actuators, intended to be used in place of the traditional bimetallic strip. NiTi actuators produce not only a greater force than the bimetal, but over a larger range and with a narrower window of temperature actuation and have been used for many applications such as green house window openers, anti-scald mixing taps and air conditioning flow controllers [21,22]. More recently, NiTi thin films have been investigated as potential microactuators [23–25] from micro-valves to micro-positioners for laser mirrors. Crucial to all these devices is control of the martensitic to austenitic transformation temperature.

The martensitic–austenite transformation temperatures can be readily obtained by bulk methods such as DSC and thermomechanical methods, neither of which is readily adaptable for thin coatings, due to a requirement of sufficient sample mass or limitations imposed by the substrate. Sheet resistance measurements or thermal XRD may be used on relatively large areas of thin film coatings but this does not meet the requirements of the electronics industry. We propose a method that offers the potential of in situ determination by SThM of these transformation temperatures at the micron level, as required by such applications. Therefore, in this report we present preliminary findings that explore the possibility of using micro-TA to study NiTi near equi-atomic shape memory alloy (SMA) thin films. The results were compared with DSC of the same material, removed from the substrate.

2. Experimental methods

Silicon substrates were deposited with near equi-atomic NiTi using a plasma assisted sputtering apparatus with a 63 mm diameter magnetron target. The operating pressure was 3 mTorr (4×10^{-3} mbar) argon, with a target power of 50 W DC for a period of 5 h. Composition control was facilitated by the addition of CP titanium on the NiTi target surface. Following deposition, half of the samples were heat treated at 600 °C for 30 min in argon to crystallise the samples. The stoichiometric ratio was determined by EDX to be 49.9 at.% Ni in Ti.

Both as-deposited and crystallised samples were ultrasonically cleaned in acetone prior to subsequent examination by thermal analysis. For DSC analysis, sputtered film samples were removed from their substrates by peeling, cut into small squares ~4 mm × 4 mm (representing a sample mass of 3–5 mg) and placed into aluminium sample pans upon which lids were crimped on.

DSC analysis (Perkin Elmer DSC-7) was carried out between −100 and 150 °C to obtain the transformation temperatures of the NiTi alloy samples. A constant rate of heating and cooling was maintained at 10 °C min^{-1}. The calorimeter was calibrated using an indium standard.

Micro-TA was carried out on a μTA^{TM} 2990 (TA Instruments). Images of topography and thermal

conductivity were obtained for both amorphous and crystallised samples above room temperature. The probe was then positioned on selected points to collect the sensor and power signals. The thermal scans were realised from room temperature up to 120°C at a constant rate of 10 °C s^{-1}. Prior to thermal scans, the probe temperature was calibrated using four certified standard samples. To reduce possible environmental interference, a damping table under the stand and an insulating cover on the top of the scanning head were used during data acquisition. The derivative curves of the LTA signals were smoothed to remove instrumental noise using Universal Analysis software attached to the technique.

3. Results and discussion

3.1. DSC analysis

Fig. 1 shows a typical DSC thermogram of an as-deposited NiTi thin film. There were no thermal events observed as expected since the as-sputtered films without heat treatment are amorphous in nature. The crystallisation temperature is between 470 and 500 °C as determined from previous DSC analysis [26]. The sample films were then subjected to a heat treatment above the crystallisation temperature. The subsequent DSC results, Fig. 2, give the following transformation temperatures for the heating part of the

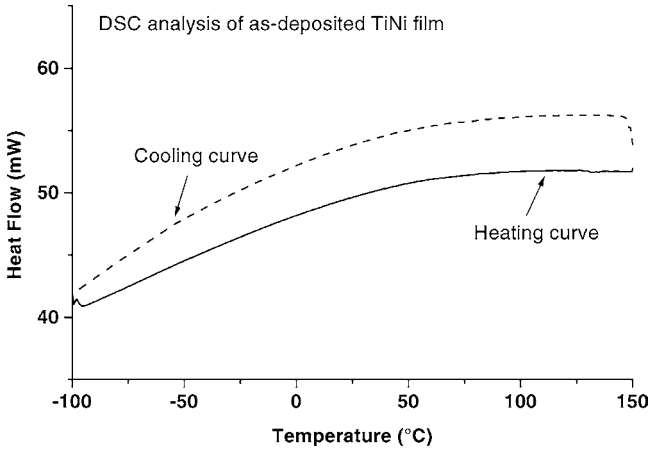

Fig. 1. DSC thermogram for the as-deposited amorphous NiTi thin film.

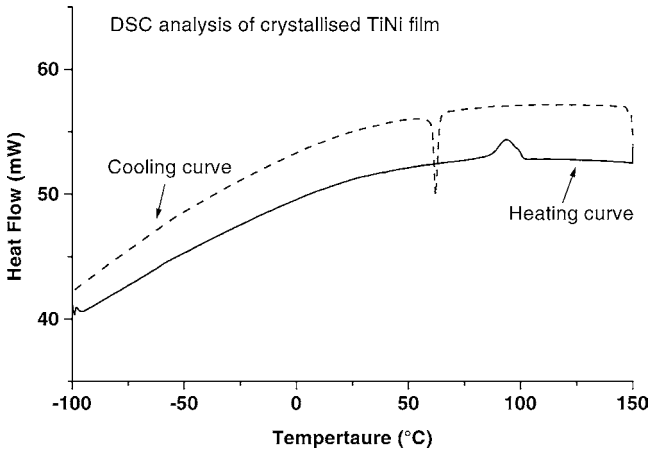

Fig. 2. DSC thermogram for the crystallised sample.

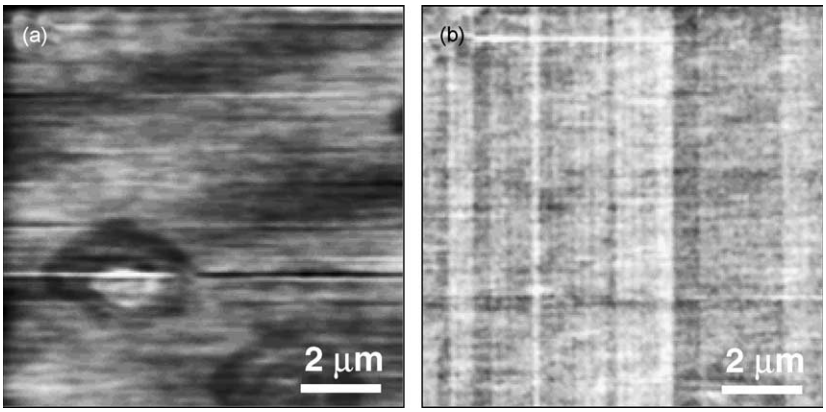

Fig. 3. Simultaneously acquired SThM topographic (a) and thermal conductivity (b) analysis data of the as-deposited NiTi thin film. Contrast in (b) is due to instrumental noise, apparent due to the low range of the power scale. The images are 10 μm × 10 μm, and have a *z*-scale of 25 nm and 0.02 mW, respectively. Probe temperature was held at 120 °C.

cycle as $A_S = 80\,^{\circ}C$, peak $= 95\,^{\circ}C$, $A_F = 102\,^{\circ}C$, where A_S and A_F are the austenitic start and finish temperatures, respectively. The DSC results confirm that crystallisation had successfully taken place in the amorphous film samples by heat treatment.

3.2. Micro-thermal analysis

Fig. 3 shows a topographic (a) and simultaneously obtained thermal (b) image of an as-deposited NiTi thin film. Fig. 4(a) and (b) are the corresponding results of the crystallised sample. The topographic image in Fig. 3(a) reveals that the surface of the as-deposited NiTi film was very smooth. By comparison, the crystallised film surface shown in Fig. 4(a) was much rougher with the appearance of raised features. However, these raised features are large (2–3 μm) compared with the crystal grain size of the NiTi films as determined from both TEM and XRD analysis to be 50–200 nm [26]. This is due to an imaging artefact peculiar to proximal probe-based microscopies, whereby the image produced is a convolution of probe and sample topography. When probe dimensions are of a similar size or larger than the features of interest in the sample topography then this effect is particularly severe. Since as stated the thermal probe has a nominal

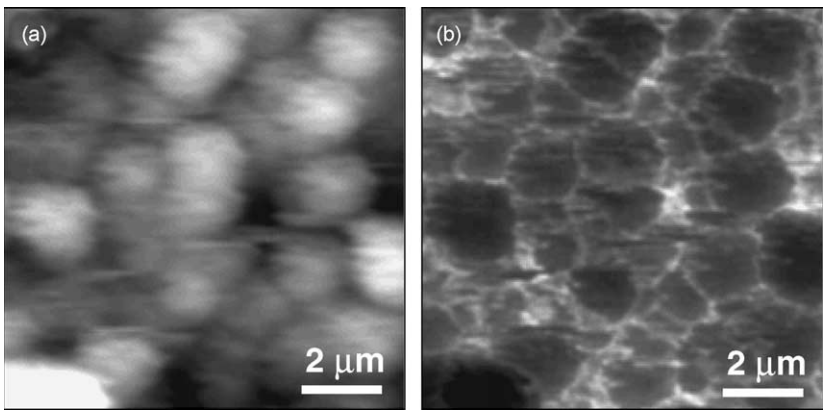

Fig. 4. Simultaneously acquired SThM topographic (a) and thermal conductivity (b) analysis data of the crystallised NiTi thin film. The images are 10 μm × 10 μm, and have a *z*-scale of 210 nm and 0.1 mW, respectively. Probe temperature was held at 60 °C.

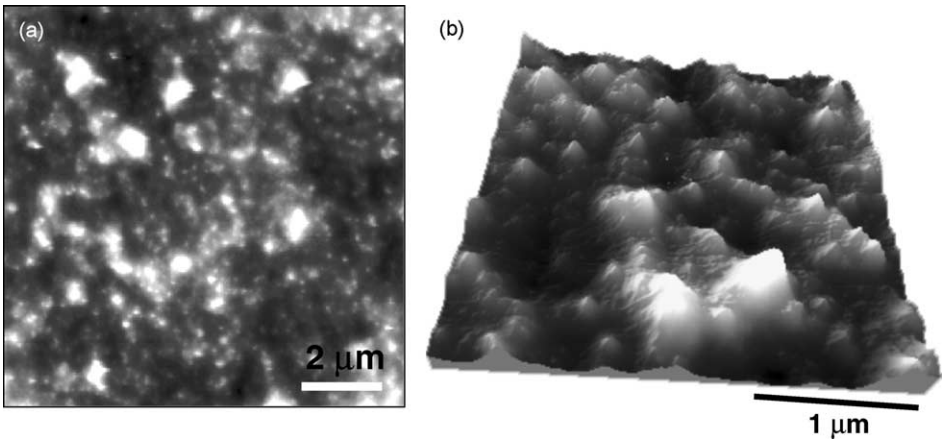

Fig. 5. AFM topography imaging revealing the accurate grain structure of the crystallised NiTi thin film consistent with TEM and XRD analysis [25]. (a) 10 μm × 10 μm and a vertical *z*-scale of 250 nm. (b) 3D visualisation of a 3 μm × 3 μm region, *z* scale of 170 nm.

terminal radius of around 500 nm, then this accounts for the loss of resolution of the alloy grains. It is possible to assess the effect of tip geometry by utilising 'blind' deconvolution routines developed by Villarrubia [27] and Williams et al. [28] and available commercially (Image Metrology ApS). For the topography data in Fig. 4(a) this procedure revealed a SThM probe with an apex radius of around 300 nm with greater than 70% of the topographic image data being due to multiple tip–sample contacts (i.e. artefactual). The use of a sharper probe allows an accurate determination of grain size and morphology consistent with TEM and XRD analysis [26], as indicated by the AFM data in Fig. 5.

Regarding the thermal images, the situation becomes more complex. For the amorphous film, shown in Fig. 3(b), there is no contrast observed even with probe temperatures as high as 120 °C (note the low power range of the thermal data). This is indicative of a smooth amorphous surface in which the texture details are beyond the sensitivity and resolution of the SThM imaging capability. In contrast, a large difference in thermal data was identified in the crystallised sample, Fig. 4(b) in which the raised features described above are clearly visible. However, care must be exercised to interpret this data since the thermal images can contain topography-related information due to variation in probe–sample contact area and hence heat flow [19]. Comparison of Fig. 4(a) and (b) indicates that the high areas in the topography correspond generally to the low thermal conductivities and vice versa. This is likely to be caused by changes in tip–sample contact area as dealt with in the above discussion of the topographic data. As a result, the measured thermal conductivity artificially increased or decreased rather than reflecting the real property of the material. The inherent problem is a relatively large terminal radius of the thermal probe used (ca. 300 nm). Therefore, it is uncertain if the thermal conductivity images obtained are related to the true thermal properties of the NiTi thin films.

In LTA measurements, power and sensor signals can be simultaneously acquired as a function of temperature. The power signal, equivalent to micro-differential thermal analysis (μDTA), measures the relative energy required to keep a constant temperature ramping rate of the probe. The sensor signal, termed as micro-thermomechanical analysis (μTMA), determines the vertical displacement of the probe relative to its original position during temperature scanning. Fig. 6 displays a typical μDTA scan for the as-deposited and crystallised film. The straight lines of the μDTA curves on the amorphous scan indicate that no heat was absorbed during the heating scans, which is in good agreement with the DSC result, Fig. 1. As stated earlier, this is because no phase transition is expected in the amorphous sample. The μTMA scan, Fig. 7 is also in agreement with the DSC for the amorphous sample with no evidence of a crystal transformation. The linear increase in the

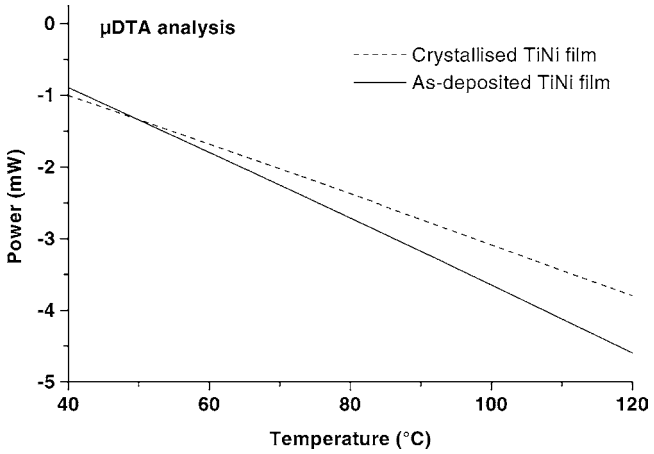

Fig. 6. Typical μDTA traces for the as-deposited and crystallised NiTi thin film sample.

sensor displacement with temperature resulted from the thermal expansion of sample and tip.

Fig. 6 also gives a representative μDTA of the crystallised NiTi film. It is very difficult to find if there is any change on a power signal curve, due to the amount of heat involved in the reverse transformation being very small, combined with the small volume (ca. 0.6 μm^3 estimated from the calculated probe radius of 300 nm) of the materials sampled in LTA measurements. However, when the power signal is differentiated with respect to temperature, a downward peak can be clearly seen on the derivative power curve, Fig. 8, indicating that the martensite to austenite transition had indeed occurred. It is also clear that the sensor responded to the phase transformation in the corresponding μTMA curve, Fig. 7. The curve initially goes up in an approximately linear fashion, followed by a sudden drop at a temperature consistent with the martensite to austenite transition, finally it resumes its upward linearity. In its derivative curve, there is a downward peak in the corresponding region. This was repeated for 59 different locations, of which nine representative traces are presented in Fig. 9. It is reasonable to believe that this abrupt deviation from linearity or contraction in dimension is closely associated with the transformation from martensite to austenite.

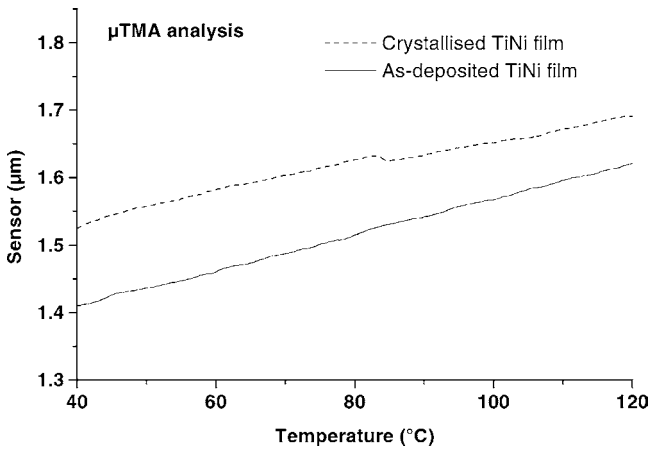

Fig. 7. Typical μTMA traces for as-deposited and crystallised NiTi thin film samples.

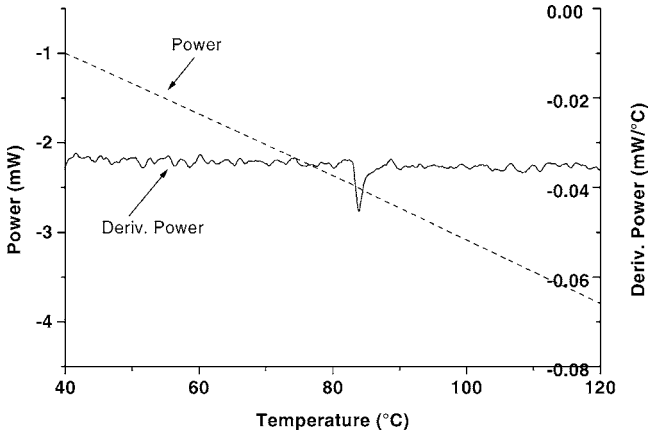

Fig. 8. μDTA and differentiated μDTA results for the crystallised NiTi thin film sample.

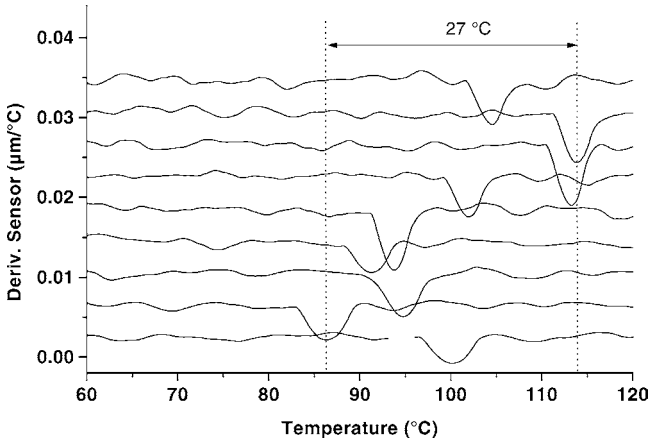

Fig. 9. Differentiated μTMA traces for nine representative test locations on the crystallised NiTi thin film sample.

Firstly, this is supported by the fact that such a volume change did not happen to the as-deposited sample as it was in an amorphous state. Secondly, comparison of Figs. 7 and 8 demonstrate that the dimension change and endotherm occurred simultaneously, implying that the former was not caused by some other processes.

The average value by which the sensor signal changed on transformation, obtained from 59 separate test locations and expressed as a percentage of film thickness ($5 \pm 0.25\,\mu m$) was $0.44 \pm 0.02\%$ [26]. Assuming that the unit cell contracts equally in all directions on transformation, the linear contraction $(\Delta l/l_0)$ can be expressed as

$$\left(\frac{\Delta l}{l_0}\right) \cong \frac{1}{3}\left(\frac{V_M - V_A}{V_M}\right) \quad (1)$$

where V_M and V_A are the volumes of the martensitic and austenitic unit cells, respectively (54.63 and $53.89\,Å^3$, from JC-PDF files 18-899 and 27-344). Using this calculation, the theoretical linear contraction on transformation is 0.45%, which is in excellent agreement with the μTMA results.

The finding in the current study is also consistent with a recent report, in which Uchil et al. [29] employed a conventional TMA to measure the thermal

expansion of a Nitinol wire of 2.4 mm in diameter and 8 mm in length. It is therefore concluded that the point of discontinuity in the sensor deflection can be assigned as a temperature at which the transformation to austenite takes place. The material was martensitic below this temperature, and austenitic above this temperature.

It should be noted that the sensor response to the NiTi SMA is markedly different from that observed in polymers that have been used as the main materials in previous SThM studies [19]. When the probe temperature reaches the glass transition, or melting temperature of polymers, the probe will sink into the samples due to their elastic moduli being reduced dramatically by two or three orders of magnitude [16]. This often results in a permanent damage, such as a crater-like pit at a sampling location. However, it was not the case for the NiTi thin film in the current study. This is because the martensitic transformation is a thermoelastic reversible process. Once the sample transforms back to the martensitic phase on cooling, the volume change during the transition will recover. This is evidenced by the fact that no visible change was found on the SThM sampling points using high resolution AFM.

Comparison of Figs. 7 and 8 also indicates that the sensor signal is more sensitive than the power one. In some cases of LTA measurements, it was difficult to observe a distinctive peak on the derivative of the power signal as noise was significant around the transition region. Such noise pollution may result from disturbance due to surrounding environments, for example, air currents. However, the probe deflection received a less adverse effect since it measures the position rather than heat exchange.

Comparison of 59 LTA measurements on different locations of the heat treated sample showed some variation of the observed transformation temperature, from approximately 83–110 °C for A_S, with the modal value being about 104 °C. It is considered that this was less likely to have been caused by experimental errors as the melting temperatures of crystals for calibration deviated only within about 5 °C after many repeated measurements. Instead, the shift in temperature might be attributed to an inhomogeneous distribution of Ti and Ni in the thin films since a tiny amount of change in the proportion of these two elements will result in NiTi SMAs with a large difference in transition temperature. For example, there is a 100 K temperature change in transformation temperature between 50 and 51 at.% Ni in Ti. Otsuka and Ren [30] have already pointed out this problem in the practical control of NiTi thin film quality prepared by a sputtering technique. In this sense, LTA offers the possibility of detecting such fluctuations of chemical composition within a single sample.

In contrast to the range of transition temperatures observed with micro-TA, only one transition was determined with DSC (Fig. 2). This is because DSC assesses the sum of the properties of the film as opposed to localised information being collected by micro-TA. The results from the two methods may not be contradictory if one looks carefully at the DSC curve of Fig. 2. A wide transition region of curve between 80 and 102 °C may signify the inhomogeneous nature of the sample material. The span of this region is also coincidentally similar to the scale (83–110 °C) of the temperature variation in LTA. However, a difference of 5 °C in the absolute values of these two temperature ranges was noticed. At present, the reasons for this are not entirely clear; but the large difference in thermal properties between the metallic sample film and materials for SThM calibration may partly account for this. The identification of new calibrants suitable for metallic samples is beyond the scope of this work, however, it should be noted that it is likely that standards based upon indium (as used for DSC) or eutectic solders are likely to contaminate the SThM probe during sample melting and hence not be suitable.

4. Conclusions

NiTi SMA thin films have been studied for the first time by employing micro-TA. The results demonstrate that both power and sensor signals can be used to characterise the phase transformation temperatures. The latter is more sensitive than the former possibly because the probe deflection is less disturbed by surrounding environments. The austenitic transformation temperatures are, respectively, identified as a sudden decrease and increase in the probe deflection with an associated sample contraction of 0.44%. The dimension change of the materials during the phase transformation can be explained by the difference in the unit cell volumes of the different phases. In addition, a

large variation of the transition temperatures detected suggests an inhomogeneous distribution of Ti and Ni in the sputter-prepared thin films. This is currently under further investigation.

Acknowledgements

We thank the EPSRC, UK, for funding for JZ and of the μTA™ 2990 microscope under the Multi-Use Equipment Initiative, and also for funding NWB via a studentship.

References

[1] C.C. Williams, H.K. Wickramasinghe, Appl. Phys. Lett. 49 (1986) 1587.
[2] M. Nonnenmacher, H. Wickramasinghe, Appl. Phys. Lett. 61 (1992) 168.
[3] A. Majumdar, J.P. Carrejo, J. Lei, Appl. Phys. Lett. 62 (1993) 2501.
[4] R.B. Dinwiddie, R.J. Pylkki, P.E. West, in: T.W. Tong (Ed.), Thermal Conductivity 22, Technomics, Lancaster, PA, 1994, p. 668.
[5] A. Hammiche, M. Reading, H.M. Pollock, M. Song, D.J. Hourston, Rev. Sci. Instrum. 67 (1996) 4268.
[6] A. Hammiche, D.J. Hourston, H.M. Pollock, M. Reading, M. Song, J. Vac. Sci. Technol. B 14 (1996) 1486.
[7] M. Reading, Trends Polym. Sci. 1 (1993) 248.
[8] D.M. Price, M. Reading, A. Caswell, A. Hammiche, H.M. Pollock, Microsc. Anal. 65 (1998) 17.
[9] D.M. Price, M. Reading, T.J. Lever, J. Therm. Anal. Cal. 56 (1999) 673.
[10] D.M. Price, M. Reading, A. Hammiche, H.M. Pollock, J. Therm. Anal. Cal. 60 (2000) 723.
[11] D.M. Price, M. Reading, A. Hammiche, H.M. Pollock, Int. J. Pharm. 192 (1999) 85.
[12] P.G. Royall, D.Q.M. Craig, D.M. Price, M. Reading, T.J. Lever, Int. J. Pharm. 192 (1999) 97.
[13] G.H.W. Sanders, C.J. Roberts, A. Danesh, A.J. Murry, D.M. Price, M.C. Davies, S.J.B. Tendler, M.J. Wilkins, J. Microsc. 198 (2000) 77.
[14] L. Bond, S. Allen, M.C. Davies, C.J. Roberts, A.P. Shivji, S.J.B. Tendler, P.M. Williams, J. Zhang, Int. J. Pharm. 243 (2002) 71.
[15] H.M. Pollock, A. Hammiche, M. Song, D.J. Hourston, M. Reading, J. Adhesion 67 (1998) 217.
[16] V.V. Gorbunov, N. Fuchigami, V.V. Tsukruk, High Perform. Polym. 12 (2000) 603.
[17] R. Häßler, E. zur Mühlen, Thermochim. Acta 361 (2000) 113.
[18] V.V. Gorbunov, N. Fuchigami, J.L. Hazel, V.V. Tsukruk, Langmuir 15 (1999) 8340.
[19] H.M. Pollock, A. Hammiche, J. Phys. D 34 (2001) R23–R53.
[20] W.J. Buehler, J.V. Gilfrich, R.C. Wiley, J. Appl. Phys. 34 (1963) 1475.
[21] T.W. Duerig, Mater. Sci. Forum 56 (1990) 679.
[22] H. Ohkata, H. Tamura, Mater. Res. Soc. Symp. Proc. 459 (1997) 345.
[23] E. Makino, T. Mitsuya, T. Shibata, Sens. Actuators A 79 (2000) 251.
[24] E. Makino, T. Mitsuya, T. Shibata, Sens. Actuators A 79 (2000) 128.
[25] A.D. Johnson, J. Micromech. Microeng. 1 (1991) 34.
[26] N.W. Botterill, Deposition and characterisation of thin film nickel–titanium shape memory alloys for microactuation, Thesis, University of Nottingham, 2002.
[27] S. Villarrubia, J. Natl. Inst. Stand. Technol. 102 (1997) 435.
[28] P.M. Williams, K.M. Shakesheff, M.C. Davies, D.E. Jackson, C.J. Roberts, J. Vac. Sci. Technol. B 14 (1996) 1557.
[29] J. Uchil, K.P. Mohanchandra, K. Ganesh Kumara, K.K. Mahesh, T.P. Murali, Physica B 270 (1999) 289.
[30] K. Otsuka, X. Ren, Intermetallics 7 (1999) 511.